AMPLITUDE VERSUS OFFSET (AVO) AN EMERGING TOOLS FOR MINERAL EXPLORATION, IN THE BASEMENT COMPLEX: CASE STUDY OF ZARIA, NORTH CENTRAL NIGERIA.

I. B. Osazuwa and *Collins C. Chiemeke
*Corresponding Author
Physics Department, Ahmadu Bello University, Zaria, Kaduna State, Nigeria.
E-Mail: dondigital2002@yahoo.com Mobile phone +2348035780638

Abstract

The mining industry has traditionally used geologic field mapping, electromagnetic and potential field techniques, and drilling to explore for new mineral deposits, but with new discoveries of large near-surface deposits becoming increasingly rare and the known reserves of most economic minerals in decline, it is clear that new deep exploration techniques are required to meet the future needs of industry and society. With gravity and magnetic methods unable to resolve targets beyond about 500 m, high-resolution seismic reflection techniques similar to those used by the petroleum industry, but modified for the hardrock environment, show the greatest potential for extending exploration to depths of 3 km, the current maximum depth of mining. A high resolution seismic technique has recently been carried out in Zaria to delineate and characterise the structures and lithologies within the batholith using AVO analysis. The geology of Zaria revealed that it is made up of Precambrian rocks that consist of granite that form the major part of the batholiths along with low grade meta-sediments and gneisses that constitute the country rock into which the granitic batholiths intruded. The results of the AVO analysis showed a general trend of increase of amplitude with offset. Three AVO types were identified, which include type -3 that corresponds with occurrence of sills, type -4 that corresponds with the occurrence of granite and gneisses and type -5 that identified the occurrence of fracture basement. The effectiveness in the identification of the various lithologies and structures showed that AVO will serve as an effective tool for mineral exploration in the nearest future.

Introduction

Most economic mineral deposits are found in hard-rock, rather than sedimentary environments. Since the impedance contrasts and reflection coefficients between most common igneous and metamorphic rocks are smaller than those between sedimentary rocks ($R \sim 0.1$ vs. 0.3), the signal-to-noise S/N ratio in minerals surveys will be low, making it more difficult to image structures in the country rock. Particular care must thus be taken during acquisition and processing of seismic data to maximize the S/N ratio. By careful testing of different sources before conducting the survey itself, and by maximizing the fold, (Eaton et al., 2003).

2-D surveys have successfully detected and imaged large massive sulphide deposits such as the magmatic and volcanic massive sulphide (VMS) deposits (Matthew and David, 2008).

Amplitude variation with offset (AVO) comes about from something called 'energy partitioning'. The amplitudes of the reflected and transmitted energy depend on the contrast in physical properties across the boundary (Michael et al, 2002).

Knott (1899) and Zoeppritz (1919) invoked continuity of displacement and stress at the reflecting interface as boundary conditions to solve for the reflection and transmission coefficients as a function of incident angle and the media elastic

properties, in what is today known as Zoeppritz Equation, mostly written as (Castanga and Milo, 1999).

$$R(\theta) = A + B\sin^2\theta + C(\tan^2\theta - \sin^2\theta) \qquad (1)$$

Where $R(\theta)$ = reflection coefficient, = incident p-wave angle, A, B, C are constants. Shuey's (1985) simplified the rather complex AVO Zoeppritz Equation, by ignoring the C term, to obtain a linear equation.

$$R(\theta) = A + B\sin^2\theta \qquad (2)$$

In this case the amplitudes at every time sample of a normal move out (NMO) gather are plotted against the squared sine of the angle-of-incidence. The intercept describes the "normal-incidence P-reflectivity" (NIP) A, while the slope is the gradient B (how the amplitude changes with angle). All current quantitative AVO methods work this way (Michael et al, 2002). Laboratory investigations have shown that strong contrast can exist between the elastic properties of massive sulphide ores and typical crystalline host rocks (Salisbury et al., 2003). These measurements indicate that seismic scattering by ores may give rise to pronounced amplitude variation with offset (AVO) (Bohlen et al 2003). Numerical modelling suggests that wave conversion and scattering are quite sensitive to the shape of the body and to changes in Poisson's ratio across interface. Since massive sulphides with similar acoustic impedances can display a wide range of Poisson's ratio values, which will make it have remarkable AVO signature relative to the host rock, it is likely that AVO and other differences in the scattering of seismic waves by ore deposits will eventually be used to estimate their composition. Given the economic importance of massive sulphides, this is a subject of much current research (Salisbury, et al, 2003).

Location of the study area

The study area (Fig. 1) is bounded by latitude 11° 13 52.37 N, longitude 7° 41 49.26' E and latitude 11° 06 16.72 N, longitude 7° 42 11.56 E. With average elevation of 650 m above sea level. The seismic reflection profile lines are shown with arrows, the direction of the arrows shows the direction of the profile. The geological map of the survey area is shown in figure 2.

Geology of the study area

The older granite outcrops in the vicinity of Zaria are exposures of a syntectonics to late-tectonic granite batholiths which intruded a crystalline gneissic basement during the Pan-African Orogeny. An innumerable small complementary shear fault pervades the batholiths on consolidation. On a regional scale the dextrally displacive NE-SW shear faults are more important as a result of their large size. But on a local scale the sinistrally displacive NW-SE shear faults are statistically more numerous, although individual sizes are small and displacements minor. It is significant that many controlled phenomena in the Nigeria basement, e.g. mineralisation, are also NE-SW orientated. The wide scatter in the foliation trends of the Zaria granite batholiths appears to have r
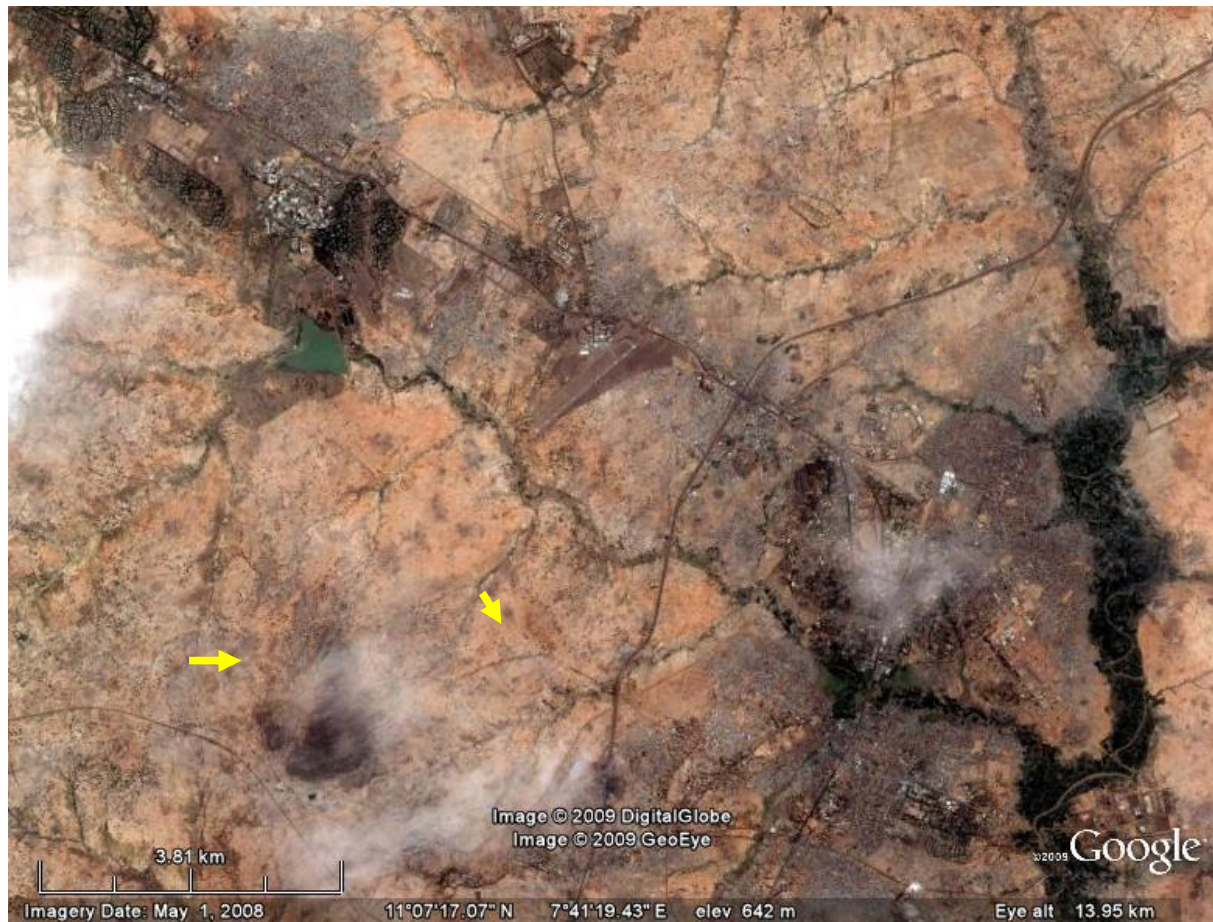
Figure 1: location map of the study area showing profile lines in red, adapter from Google earth

Data processing

The processing of the AVO data started with the importation of the raw seismic data into the ReflexW software use for both reflection and refraction seismic analysis, to convert to its format. The wrong seismic geometry (relative position of the source and receivers) entered in the field was edited. The gain filter was applied to correct for the effect of geometrical spreading and attenuation, and to enhance the weak reflection events. Frequency wavenumber (fk) filter was then applied to remove the effect of ground roll and refraction events. The processed data was subjected to semblance analysis, to generate a 2D velocity model of the subsurface. The generated velocity models was used for the dynamic correction and to sort the data into a common midpoint traces. To ascertain the depth of origin of the AVO seismic signals, the processed fk filtered data was duplicated, and time migration was applied to reposition the reflection events to their correct position, after which the migrated seismic section was converted into a depth sections using the initially generated 2D velocity model. Since the offsets (relative distances between the various shots and receivers) and depths of the AVO signals were known, it became possible to reconstruct the angle between the incident ray and the normal. This was extracted along with the amplitudes of the various traces for amplitude versus sin square incidence angle plot, that were analyzed to determine their various AVO effect in line with Shuey's equation.
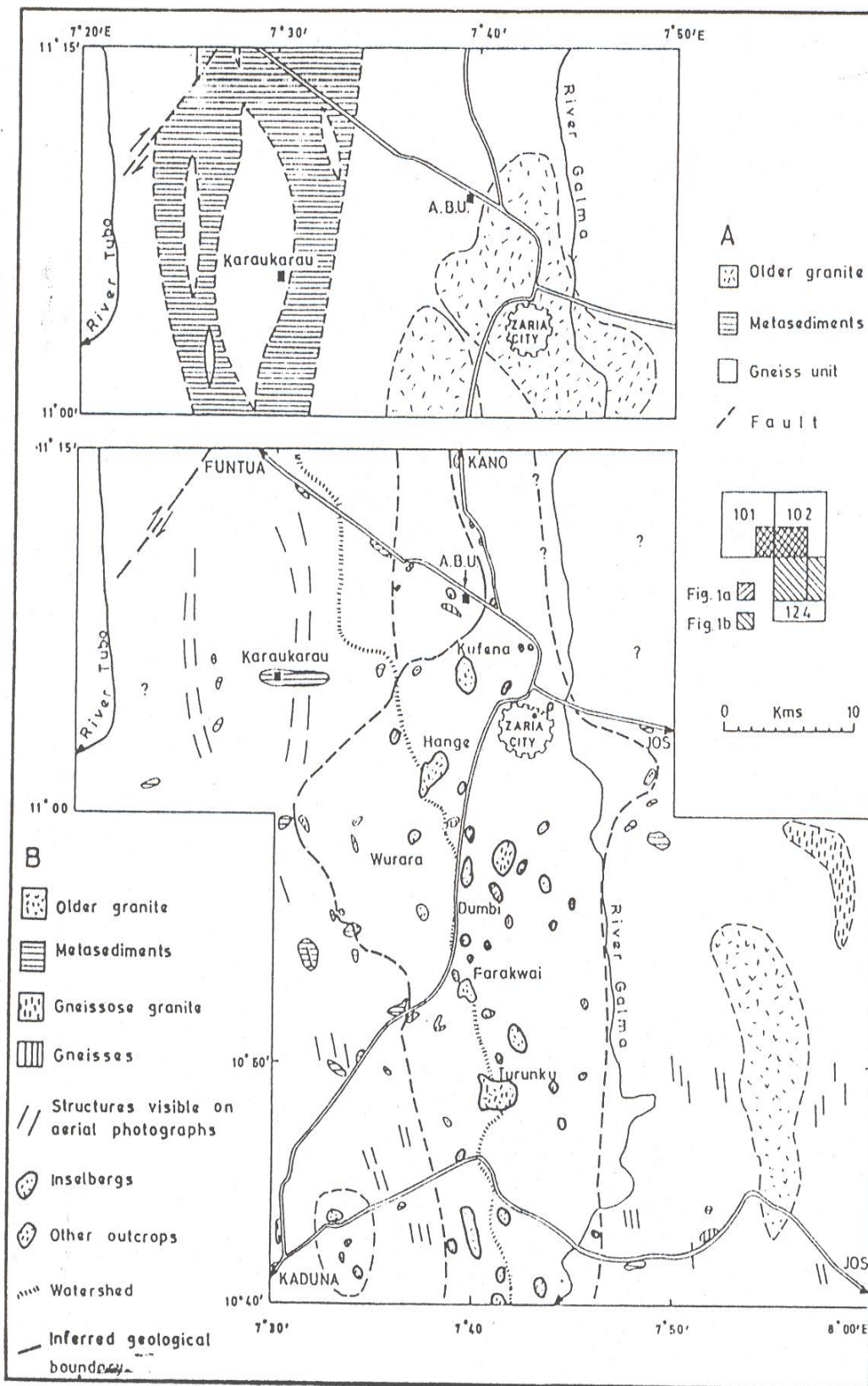
Figure 2: Geological map of Zaria Batholith and its environ, Map obtains from Geology Department A. B. U.   Zaria

Data acquisition

Data acquisition started with insertion of the geophone at 1 m intervals, with an offset distance (distance between source and first receiver) of 1 m. After each shot, the first geophone closer to the sledge hammer used as energy source was removed, and placed 1 m ahead of the last geophone. The connections to each of the take-outs were swapped in between the geophone in the forward direction, toward the direction of increasing profile. The shot was advanced forward by 1 m to occupy the position of the removed first geophone. When all the connections were completed, the shot was fired with a stack of 5. The generated seismogram was saved for onward processing. This resulted in a 12 fold common midpoint (CMP) data coverage, for the 24 channel digital seismograph used.

Results and discussion

One of the seismic profiles, profile A, was sorted into common midpoint (CMP) traces (Fig. 3a). AVO signal figure 3b was extracted from the reflection events enclosed in the rectangle, and enlarged. Qualitative analysis showed that the amplitudes of the various AVO signatures were increasing with offset. The AVO signature was traced from the depth section to have originated from a depth of 120 m. This was used in conjunction with the known offset distance to reconstruct the various angles of incidence. The amplitude of the various traces was also extracted (Table 1). The extracted amplitude was plotted against the sin square of the incidence angle in conformity with Shuey's equation (Fig. 4). The graph has a high positive intercept, which represent the normal incidence reflection and a large positive slope. This type of AVO is referred to as type -3 AVO, that has positive gradient and high positive

intercept. The high positive reflection coefficient R, ($R = Z_2 - \dfrac{Z_1}{Z_2} + Z_1$ R > 0 means Z_2 > Z_1 where Z is the impedance contrast), was clear indication that the reflection events were coming from a high density material with high impedance contrast with the surrounding rock. This could have resulted from the suspected sill material within the batholith (Fig. 5).

Profile B was also sorted into CMP traces (Fig. 6a), and the AVO signal (the Ostrand Gather) was extracted and enlarged (Fig. 6b). Qualitative analysis showed that the amplitudes were increasing with offset. The AVO signal was traced to have originated from a depth of 26 m. The known offsets were used with the depth of the origin of the AVO to reconstruct the incidence angle. The amplitude values were extracted from the various AVO traces (Table 2).

The extracted amplitudes were plotted against the sin square of the incidence angle, in line with Shuey's equation. The AVO plot, (Fig. 7), has a negative intercept with positive gradient. This type of AVO is referred to as type -5 AVO. The negative intercept

signifies negative reflection coefficient R, ($R = Z_2 - \dfrac{Z_1}{Z_2} + Z_1$ R < 0 means Z_2 < Z_1 where Z is the impedance contrast),which could have possibly resulted from the fractured basement at a depth of 26 m, identified from the borehole log sank 23 m distance along the profile (Fig. 8 and Table 3). Figure 9 indicates the possible position of origin of the AVO seismic signal from the seismic sections.

Profile C was also sorted into common midpoint traces (Fig. 10a), and the Ostrand gather of the AVO signal was enlarged, (Fig. 10b). Qualitative analysis showed that the amplitudes of the AVO signal were increasing with offset. The AVO signal was traced to have originated from a depth of 30 m. This was used in conjunction with the known offset distance to reconstruct the incidence angle (Table 4). The amplitudes of the various AVO signals were extracted. The extracted amplitudes were plotted against the square sin of the angle of incidence (Fig. 11). The graph has a positive intercept and positive gradient, which was an indication of positive reflection coefficient. The low intercept value indicates that the AVO involve is a type -4 AVO.
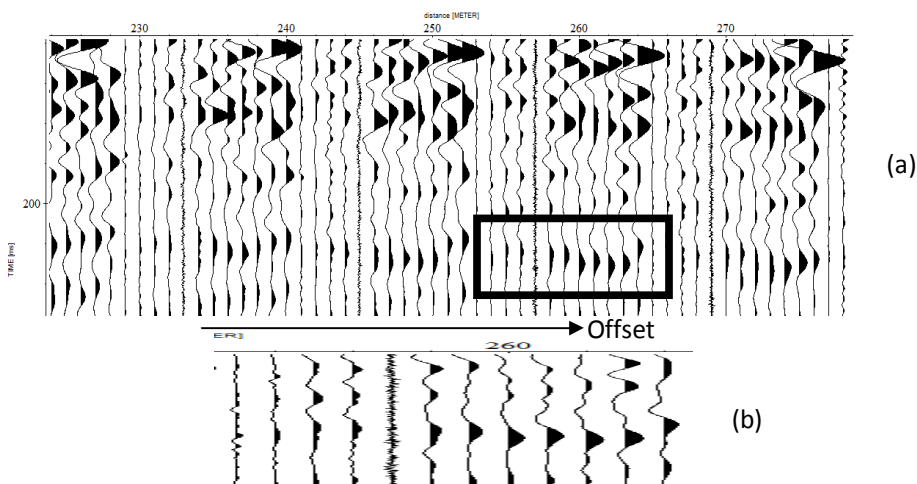
Figure 3: (a) Profile B AVO section sorted into CMP traces (b) CMP traces extracted from the AVO section

Table 1: *AVO amplitude and the incidence angles at 120 m depth for profile B*

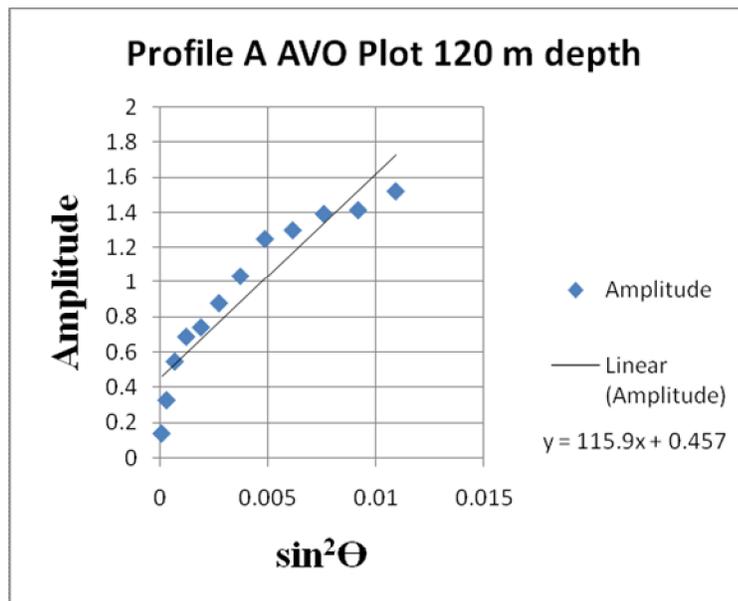| Angle (Θ) in degree	$Sin^2\Theta$	Amplitude
6	0.010926199	1.52049
5.5	0.009186408	1.4124
5	0.007596123	1.39165
4.5	0.006155829	1.29815
4	0.004865965	1.2482
3.5	0.003726924	1.0337
3	0.002739052	0.87806
2.5	0.00190265	0.74061
2	0.001217974	0.68707
1.5	0.000685232	0.54646
1	0.000304586	0.32682
0.5	0.000076152	0.1376

Figure 4: Amplitudes from each time sample of a gather at 120 m depth, from profile B plotted against the squared sine of the angle-of-incidence.
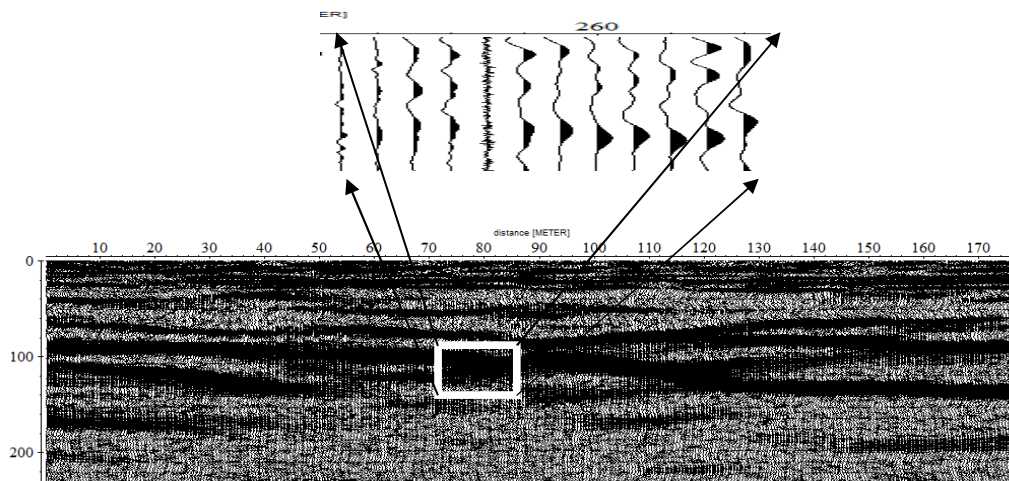

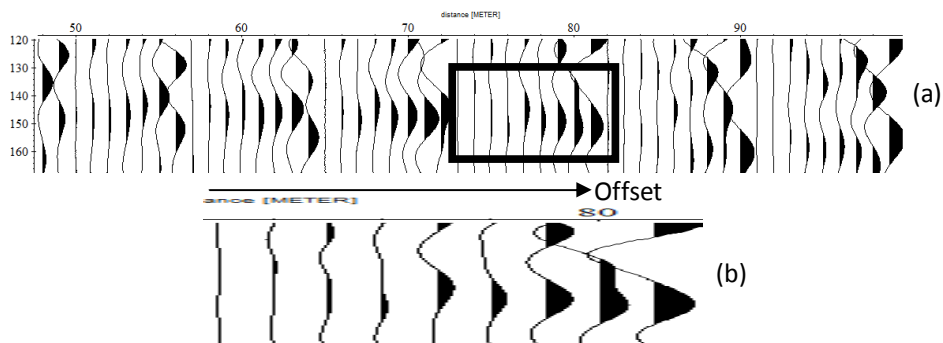Figure 5: Indication of the possible origin of AVO signal from the suspected sill

Figure 6: (a) Profile A AVO section sorted into CMP traces (b) CMP traces extracted
from the AVO section

Table 2: *AVO amplitude and the incidence angles at 26 m depth for profile A*

Angle (Θ) in degree	Sin²Θ	Amplitude
18.5	0.095491502	7.55135
16.5	0.080664716	5.16511
15	0.058526203	4.88299
13	0.046846106	2.59554
10.5	0.030153689	1.82312
8.5	0.021847622	0.99197
7	0.012814967	0.6609
5	0.004865965	0.39229
2.5	0.001217974	-0.3313
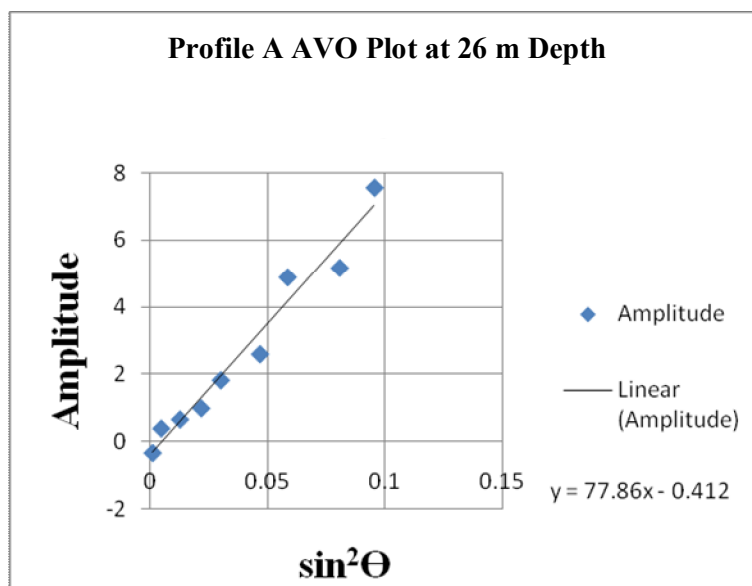
Figure 7: Amplitudes from each time sample of a gather, from profile A plotted
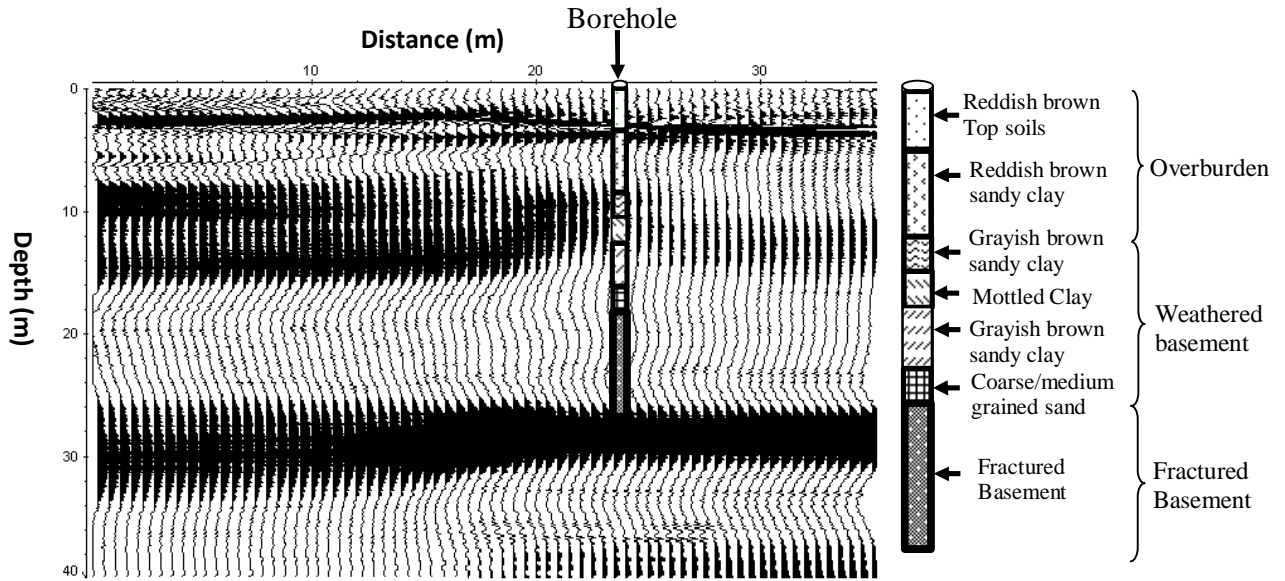against the squared sine of the angle-of-incidence.

Figure 8: Depth migrated seismic section of Profile B Borehole with borehole log

Table 3: *Profile B Lithology Borehole Log*

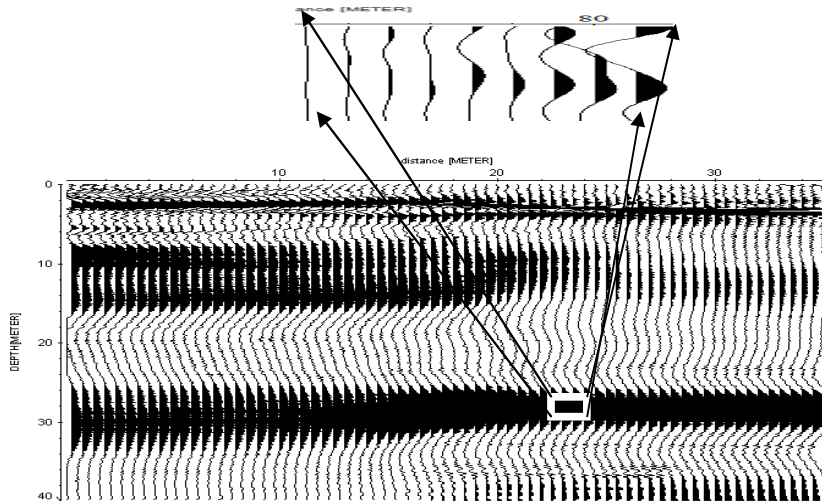| Depth (m) From	To	Thickness (m)	Interpreted Lithology	Hydrogeological characteristics
Overburden 0 – 8 m				
0	3	3 m	Reddish brown Top soils	
3	8	5 m	Reddish brown sandy clay	
Weathered Basement 8 – 18 m				
8	10	2 m	Grayish brown sandy clay	
10	15	5 m	Mottled Clay	
15	18	3 m	Coarse/medium grained sand	Aquifer
Fresh Basement 18 – 27 m				
18	27	9 m	Fractured Basement	Aquifer

Figure 9: Indication of the possible origin of AVO signal from the fractured basement
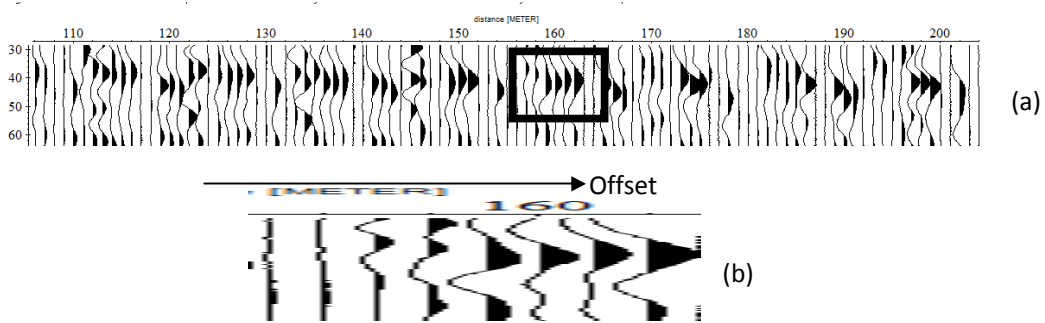

Figure 10: (a) Profile C AVO section sorted into CMP traces (b) CMP traces extracted from the AVO section

Table 4: *AVO amplitude and the incidence angles at 30 m depth for profile C*

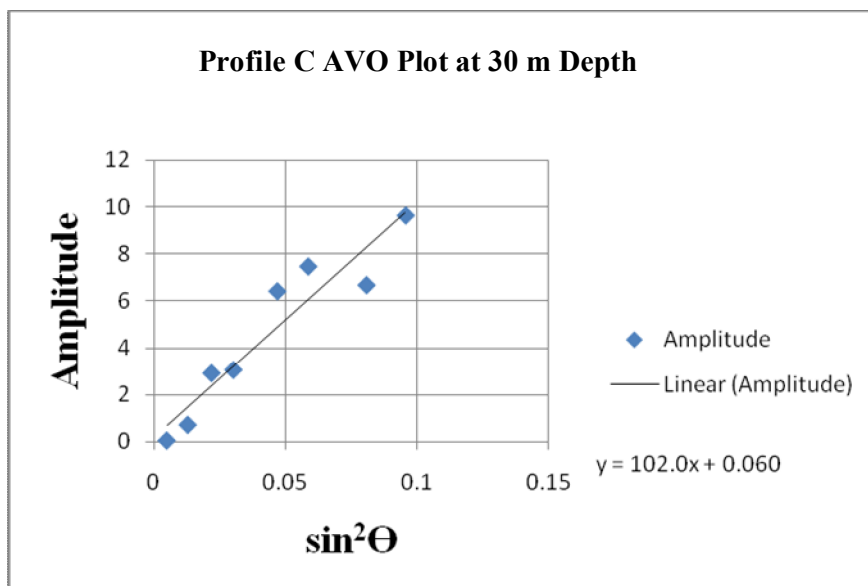| Angle (Θ) in degree	$Sin^2\Theta$	Amplitude
4	0.095491502	9.60239
3.5	0.080664716	6.65001
3	0.058526203	7.4402
2.5	0.046846106	6.38916
2	0.030153689	3.03238
1.5	0.021847622	2.89515
1	0.012814967	0.70225
0.5	0.004865965	0.03883

Figure 11: Amplitudes from each time sample of a gather at 30 m depth, from profile
C plotted against the squared sine of the angle-of-incidence.
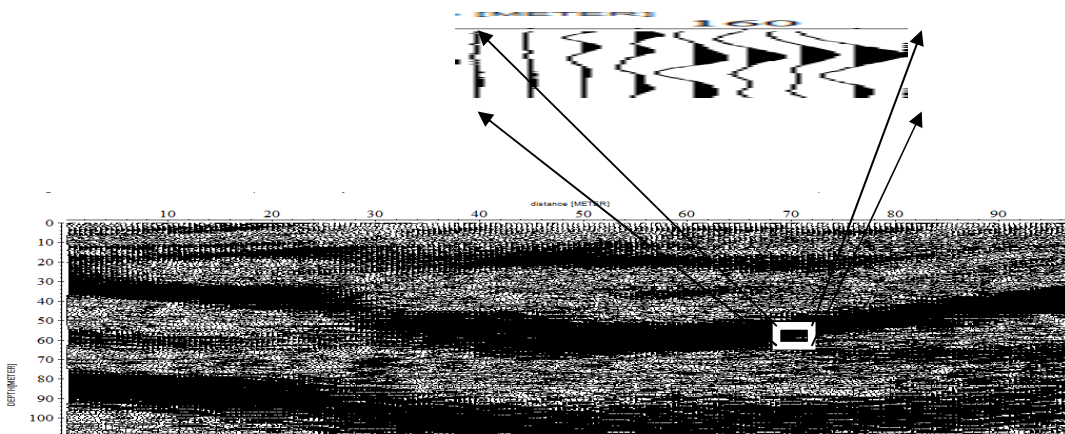

Figure 12: Indication of the possible origin of AVO signal from the contact between
gneisses and granite

The low intercept is also an indication of low impedance contrast, which might have
resulted from the contact between granite and gneisses that exist side by side along the
profile line, with very close velocity values. Figure 12 indicate the possible position of
origin of the AVO from the seismic section.

Conclusion

Comprehensive analysis of AVO signals from the high resolution seismic reflection
survey was able to identify three AVO types, which include type -3, type -4 and type -5
after the classification by Young, and LoPiccolo, 2004, corresponding to different

lithologies and structure. Type -3 was able to identify the occurrence of sill within the batholith, type -4, was able to identify the AVO signature between gneisses and granite, while the type -5 was able to identify the fracture zone within the basement. It can therefore be concluded that comprehensive AVO analysis in conjunction with high resolution seismic section will serve as an effective tool for mineral exploration within the nearest future.

Acknowledgement

References

Bohlen, T., Christof, M., and Bernd, M,. 2003. Elastic Seismic- Waves Scattering from Massive sulphide Orebodies: On the Role of Composition and Shape.

Castanga, J. P. and Milo M. B., (1999) Offset Dependent Reflectivity-Theory and Practice of AVO analysis. Society of Exploration Geophysics.

Eaton, D., Milkereit, B., and Salisbury, M., 2003. Hardrock seismic exploration; Mature technologies adapted to new exploration targets, in Eaton, D, Milkereit, B, and Salisbury, M., eds., Hardrock Seismic Exploration: Society of Exploration Geophysicists, Geophysical Development Series, v. 10.

Matthew, S., and David, S., 2008. Application of Seismic Methods to Mineral Exploration, Geological Survey of Canada.

Michael, B. Scott, P., and Calgary, 2002. Amplitude versus Offset and Seismic Rock Property Analysis: A Primer.

Salisbury, M. H., Craig W. H., and Larry M., 2003. The Acoustic Properties of Ores and Host Rocks in Hardrock Terranes, Society of Exploration Geophysics.

Salisbury, M., Milkereit, B., and Bleeker, W., 1996. Seismic Imaging of massive sulphide deposits: Part I. Rock properties: Econ. Geol., 91.

Young, R.A. and LoPiccolo, R.D., 2004. Conforming and Non-conforming Sands – An Organizing Framework for Seismic Rock Properties. Gulf Coast Association of Geological Societies Transactions, Volume 54.